Supplementary Information

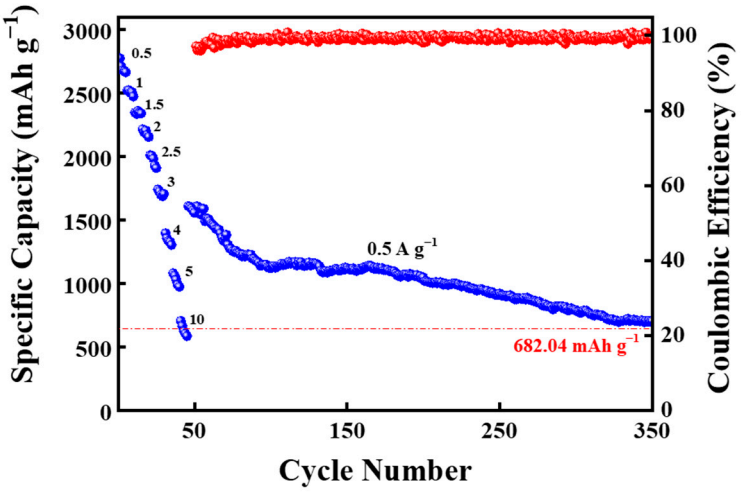

Figure S1. Electrochemical properties Si@C-CNTs/CS electrode rate performance and long cycle performance at 0.5 A g^{-1}

Figure S1 shows the rate performance curve of Si@C-CNTs/CS in the range of 0.5-10 A g^{-1} current density. Surprisingly, Si@C-CNTs/CS capacity remains at 546.47 mAh g^{-1} at A high current density of 10 A g^{-1}. The capacity can also recover to 1611.21 mAh g^{-1} when the current density changes from 10 A g^{-1} back to 0.5 A g^{-1} and remains at 682.04 mAh g^{-1} after continuing to cycle for 300 cycles.

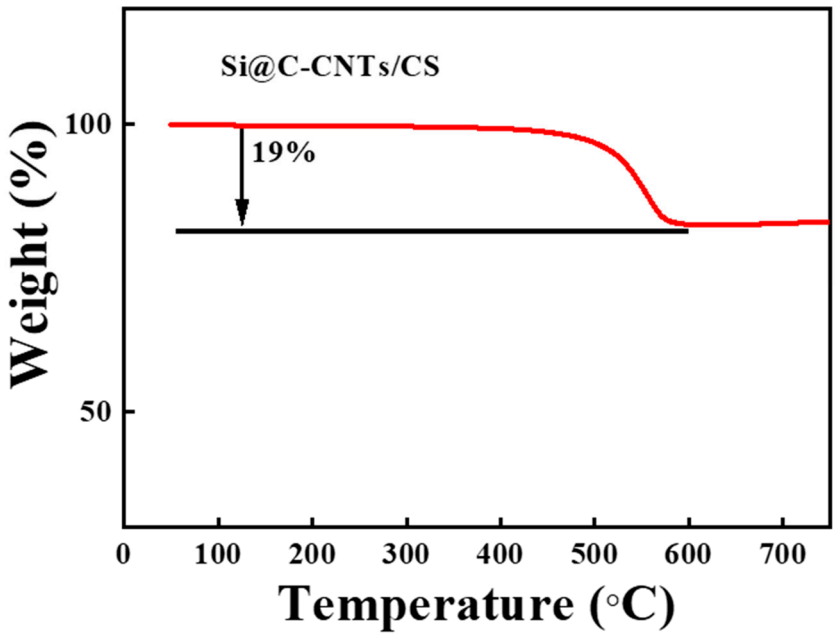

Figure S2. TGA of the Si@C-CNTs/CS.

As seen in Figure S2, the Si@C-CNTs/CS material has lost about 19% of its mass. The mass lost at 500-600°C is due to carbon decomposition, indicating that the carbon content of the composite is 19%.

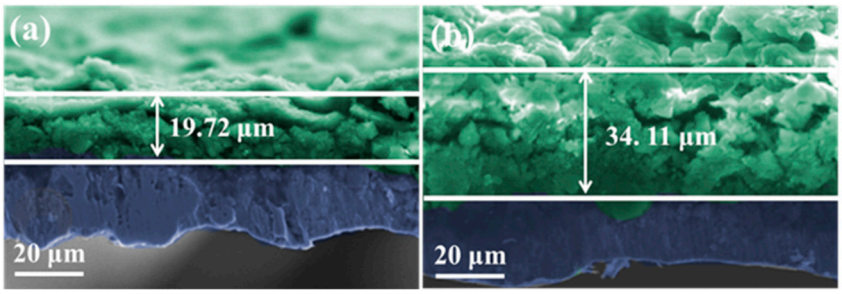

Figure S3. SEM images of pure Si (a) before initial cycle, and (b) after 100 cycles.

As can be seen from Figure S3, the volume of pure silicon negative electrode changes obviously after cycle, and the volume expansion rate is about 72.9%.

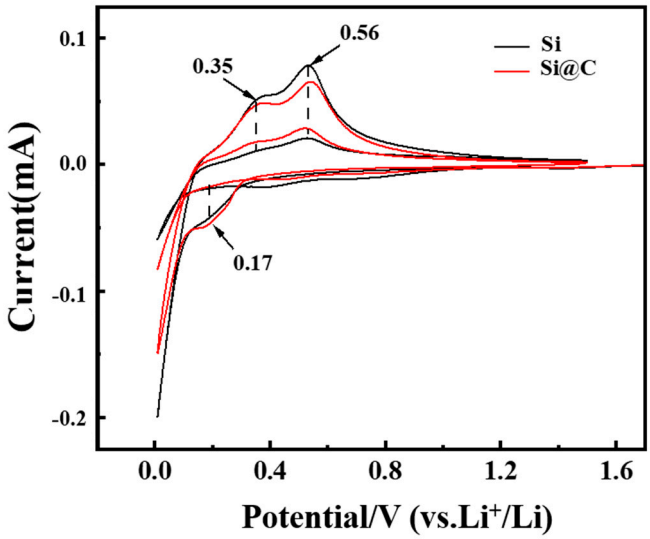

Figure S4. The first and second cycles of cyclic voltammograms of Si versus Si@C.

In Figure S4, it can be seen that there are reduction peaks in the 0.17V attachment, indicating that lithium ions are alloying with silicon to form LixSi. The oxidation peaks at 0.35V and 0.56V negative electrodes correspond to the deintercalation process of LixSi alloy

Table S1. The electrochemical performance comparisons of silicon carbon electrode in LIBs

Anodes	Cycle number	Capacity (mA h g^{-1})	Initial coulombic efficiency (%)	Refs
Si@C-CNTs/Cs	300	1487.71	77.1	this work
Si@SiO2@C@SiO2	200	1113	71	40
Si-CNT/G	100	1100	58	41
Si@C@CNT	200	1210	63	42
Si-CNF	300	799.5	74.4	43
Si-SCNT	100	1449	85	44

According to the literatures in the table, the designed material of Si@C/CNTs/CS exhibited the excellent electrochemical performance. The main reason is that the double-layer carbon mesh structure containing carbon nanotubes and carbon sheets can not only improve the electrical conductivity, but also provide mechanical flexibility and rich pore structure, which is benefited to alleviate the expansion of volume during cycling processes. The excellent cycling stability, high reversible capacity, and high electrochemical stability observed demonstrate the potential of Si@C-CNTs/Cs as a practical and high-performance anode material for LIBs. Therefore, this study can provide a valuable guideline on the designation of novel Si-base anode for improving the performance of LIBs.

References

[40]. Hu, L.; Luo, B.; Wu, C.H.; Hu, P.F.; Wang, L.Z.; Zhang, H.J. Yolk–shell Si/C composites with multiple Si nanoparticles encapsulated into double carbon shells as lithium–ion battery anodes, J. Energy Chem 2019, 32, 124–130.
[41]. Cai, H.Y; Han, K.; Jiang, H.; Wang, J.W.; Liu, H. Self–standing silicon–carbon nanotube/ graphene by a scalable in situ approach from low–cost Al–Si alloy powder for lithium ion batteries, J. Phys. Chem. Solid 2017, 109, 9–17.
[42]. Zhu, X.; Choi, S.H.; Tao, R.; Jia, X.L.; Lu, Y.F. Building high–rate silicon anodes based on hierarchical Si@C@CNT nanocomposite, J. Alloys Compd 2019, 791, 1105–1113.
[43]. Jin, Y.M.; Ai, Z.Q.; Song, Y.; Zhang, X.W.; Shi, J.L.; Ma, C. Enhanced lithium storage performance of Si/C composite nanofiber membrane with carbon coating as binder-free and self-supporting anode for lithium-ion battery, Materials Research Bulletin 2023, 167, 112429.
[44] Zhang, M.X.; Zhao, L.; Sun, D.; Sun, Y.K.; Xu, C.M.; Lu, S.C.; Li, T.; Li, Y.F.; Xiao, Z.H. S doped CNTs scaffolded Si@C spheres anode toward splendid High-Temperature performance in Lithium-ion Battery, Applied Surface Science 2023, 626, 157254.